

NUMERICAL AND EXPERIMENTAL CRUSHING BEHAVIOUR INVESTIGATION OF EBM PRINTED AUXETIC CHIRAL LATTICES

**Kadir Gunaydin^{†‡*}, Francesco G. Gallina^{†¶}, Alessandro Airoidi[†], Giuseppe Sala[†] and
Antonio M. Grande[†]**

[†] Department of Aerospace Science and Technology
Politecnico di Milano
Via La Masa 34, 20156 Milano, Italy
e-mail: kadir.gunaydin@polimi.it, web page: <https://www.aero.polimi.it/>

[‡] Aeronautics and Astronautics Faculty
Istanbul Technical University
Maslak, 80626, Istanbul, Turkey
Web page: <http://www.uubf.itu.edu.tr/>

[¶] Department of Mechanical Engineering
Politecnico di Milano
Via La Masa 1, 20156 Milano, Italy
Web page: <https://www.mecc.polimi.it/>

Key words: Chiral, Auxetic, EBM, Crushing

Abstract. In this study, Electron Beam Melting (EBM) is used to produce chiral auxetic lattices, and the compression of chiral auxetic lattice is investigated experimentally and numerically in the edgewise direction, where auxeticity can be experienced. Titanium Alloy (Ti6Al4V) metallic powder is used in this study. To understand mechanical behaviour and to characterize EBM printed parts, tensile tests are conducted. According to the tensile test results, a constitutive equation is selected, calibrated and adopted to represent the behaviour of the material. Furthermore, a chiral unit cell is manufactured and tested with a compressive load profile to investigate its displacement limit by applying large displacements without experiencing permanent deformations, degradation or failures. The same scenarios explored in the experiments are then analyzed by means of non-linear computational models using a commercial finite element code to validate a numerical approach for optimal design and performance prediction.

1 INTRODUCTION

In aeronautics, aerospace, automotive and military applications, lightweight structures such as sandwich structures have an important role considering crush resistance during impact and blast situations. For crashworthy structures, different types of sandwich structures have been proposed with different cores such as foams, lattices and trusses. The lattice cores have come forward regarding crashworthiness, and one of the most promising lattice structures are auxetic cellular solid structures [1]. Auxetic lattice structures are special structures experiencing negative Poisson's ratio so that they behave differently from conventional materials which shrinks

under a compressive load and expands under a tensile load. Amongst them chiral structures are one of the prominent auxetic structures that show -1 Poisson's ratio [2].

Chiral auxetic cellular solid was originally proposed by Prall and Lakes, and in their study -1 Poisson's ratio was proved theoretically [2]. Chiral cellular solids show anisotropic behaviour due to its asymmetric topology, and auxeticity emerges on the edgewise (in-plane) direction, thus, studies in the literature can be divided into two groups which are edgewise and flatwise (out-of-plane) studies. A certain number of edgewise studies were performed, and one of these studies includes a numerical model using dynamic shape functions to describe dynamic behaviour over a wide frequency range. A validation study was conducted to propose chiral network concept for aerodynamic applications by Spadoni et al. [3]. Chiral structures show auxeticity under small deformation however, when they are subjected to large elastoplastic deformation, they lose their auxeticity. Zhu et al. [4] used wavy ligaments to increase two mechanical properties, and as a result, the new structure showed higher energy absorption capacity. Additionally, chiral solid cellulars are proposed as a filling material for morphing structures due to their ability of undergoing large overall displacement [5, 6, 7].

In this study, EBM technology is used to produce tensile specimens and chiral unit lattice cells. In addition, EBM is used for understanding the effect of production method on mechanical properties. Specimens were produced in two different directions which are perpendicular (90°) and parallel (0°) to the powder deposition direction. Chiral lattice unit cells are produced where their flatwise surface is parallel to powder deposition direction to have higher mechanical performance and prevent additional inner support structure usage. As a result, a compression load profile is applied to the chiral unit cells, and a validation study is conducted using ABAQUS Standard.

2 METHODS

2.1 Material and Processing

Poisson's ratio of the chiral cellular solids is independent from its constituent material, however, besides the topology of the cellular solids, the constituent material is important for determining the mechanical performance for crush applications. Therefore, manufacturing method is implicitly playing a significant role in the cost, production challenges, and performance. Commercially offered metal based honeycomb structures are continuously produced from an aluminium sheet by the help of cutting and bending metal rolls [8]. The development of the additive manufacturing (AM) processes in recent years provide an opportunity to produce arbitrary topologies with less limitation comparing to conventional production methods. One of the promising AM technique is EBM additive manufacturing process that uses an electron beam to melt metallic powders [9]. Arcam A2 EBM metallic 3D printer and ARCAM Ti6Al4V ELI metallic powder have been used in this study. Titanium alloy is used due to its outstanding mechanical properties of high specific strength, high corrosion resistance, excellent biocompatibility, thus titanium alloys are prominent material for aerospace and bio-engineering fields. ARCAM Ti6Al4V ELI is a gas atomized prealloyed powder in a size range of 45-100 μm [10], the chemical specification and mechanical performance of the powder material can be seen in

Table 1 and 2.

Table 1: Chemical specifications of Arcam Ti6Al4V ELI

Aluminium	Vanadium	Carbon	Iron	Oxygen	Nitrogen	Hydrogen	Titanium
6.0 %	4.0 %	0.03 %	0.10%	0.10%	0.01%	< 0.003%	Balance

The metal powder under vacuum is melted with electron beam gun which accelerates electrons to a velocity range of 0.1-0.4 times the speed of light using heated tungsten filament by a high voltage of 60kV [11]. Consequently, electrons hit the metal powders and transfer the kinetic energy mostly as thermal energy to the metal powder, and with this energy particles melt and merge according to the energy of electron beam and layer thickness. The company suggested default building parameters with a layer thickness of 50 μm is used in this study.

Table 2: Mechanical specifications of Arcam Ti6Al4V ELI

Yield Strength	Ultimate Tensile Strength	Rockwell Hardness	Elongation	Area Reduction	Elastic Modulus
930 MPa	970 MPa	32 HRC	16%	50%	120 GPa

2.2 Chiral cellular structures

The unit cell and topology parameters of chiral hexagonal structure is shown in Figure 1 consists of equal sized nodes or cylinders joined by the ligaments, or ribs, or walls of equal length L . The outer radius of nodes are denoted by r , and the auxeticity is provided by the wrapping of the ligaments around the nodes. The extrusion length of the chiral cell is denoted by e . In the study of Prall and Lakes, nodes were considered rigid structures when obtaining negative Poisson's ratio [2]. The ligaments are connected to the nodes tangentially. However, in this design 0.5 mm fillets, f are used in the tangential constraints to prevent stress concentration. The angle of β and θ are the topology parameters, can be calculated using Equation 1, which describes the configuration of assembly and orientation of ligaments respects to the line between the center of nodes [2, 5]. Chiral geometry is significantly dominated by $\cos \beta$, and according to the studies of Spadoni et al. [12] about chiral structure filled truss-core aerofoils, the mechanical performance of the chiral structure is affected by L/R .

$$\sin \beta = \frac{2r}{R}, \tan \beta = \frac{2r}{L}, \sin \theta = \frac{R/2}{R}, \cos \beta = \frac{L}{R} \quad (1)$$

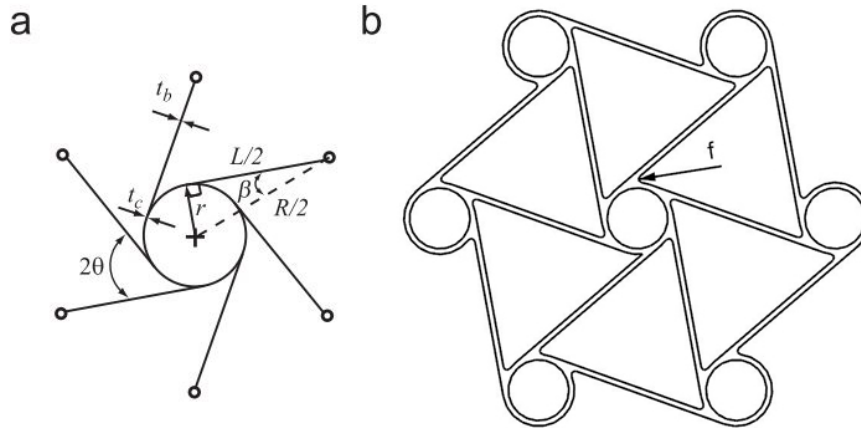


Figure 1: Geometry of a hexagonal chiral lattice: (a) topology parameters and (b) unit cell

Dimensions of the chiral unit cell are given in Table 3. It is also seen from Figure 1 that there are two thickness parameters, t_c denotes the thickness of the nodes, and t_b defines the ligament thickness. The main reason of this difference is the production method because commercially offered metal based honeycomb structures are continuously produced from an aluminium sheet by the help of cutting and bending metal rolls, and adhesion or welding of the spare plates [8]. However, the same thicknesses of nodes and ligaments can be obtained using additive manufacturing.

Table 3: Dimensions of the unit chiral cell.

R	L	r	t_b	t_c	f	e
28.77 mm	26.81 mm	5.22 mm	0.8 mm	0.8 mm	0.5 mm	16 mm

2.3 Mechanical Characterization

To understand the mechanical behaviour and characterize EBM printed parts tensile tests are conducted according to ASTM E8 with a velocity of 0.45 mm/min. Each test specimens are produced in two different directions, 0° and 90° due to characteristic anisotropic behaviour of EBM printed parts. Chiral lattice cells are produced laterally on the flatwise direction to prevent the difficulty of supports removal process and obtain higher mechanical performance in the edgewise direction. In all tests, MTS 810 Material Test System (250 max payload) is used with MTS 647 Hydraulic Wedge Grip, and MTS 634.31F-24 extensometer is used in the tensile tests. Moreover, an additional fixture is designed and produced for the chiral lattices compression tests. For the exhibition of auxeticity two upper and lower nodes supported with two cylindrical pins and bearings to free the movement of the unit chiral cell upper and lower nodes on the lateral direction and rotation on the edgewise direction.

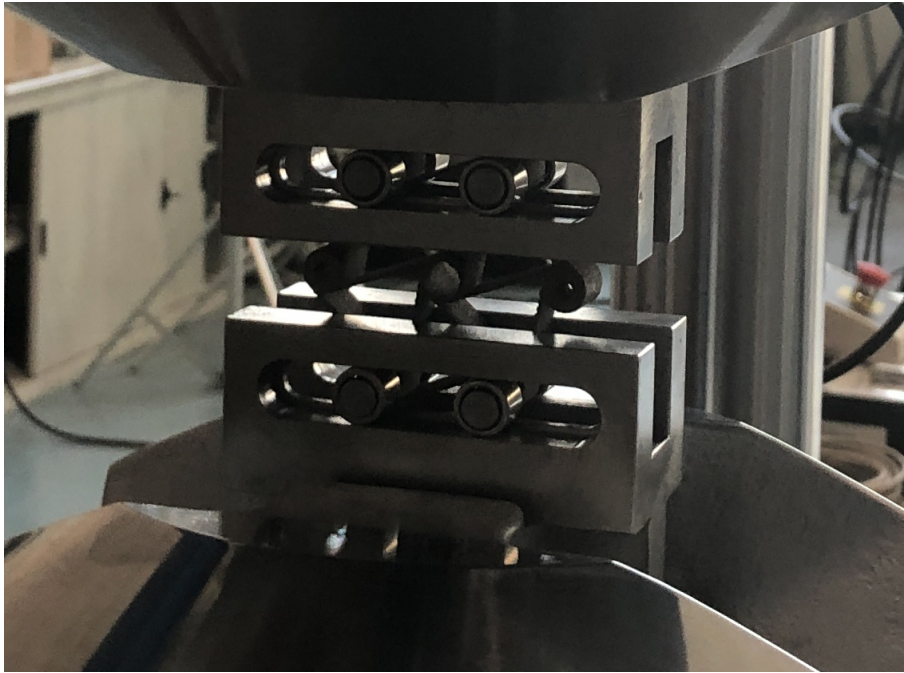


Figure 2: Fixture for chiral lattice compression

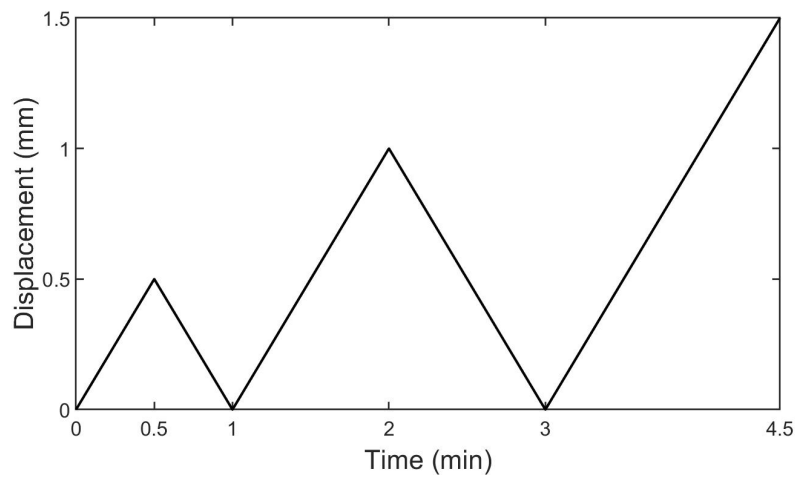


Figure 3: Compressive load profile for chiral lattices

2.4 Numerical Analysis

A three steps compressive load profile analysis of the chiral hexagonal unit cell is carried out by implicit finite element models developed using the commercial code ABAQUS 2018. The elements used for the numeric analysis are C3D20R, quadratic brick element, with reduced integration (2x2x2 integration points). The model consists of 47628 elements with an average aspect ratio of 1.70. The finite element simulation is conducted on a computer with 16 cores

and 24 GB of RAM, and the wall clock time for the simulation is 22 hours. The deformation of chiral structures are estimated using a linear material by a geometric stiffening and finite strain elements including non-linear analysis. The equilibrium is computed by the implicit Newton-Raphson method, with a fixed step of $1.661e-3$. The constituent material is considered linearly elastic, and onset of the plastic deformation is specified with the onset of the yields stress of EBM printed Ti6Al4V. Continuum distributing couplings are used in two upper and lower nodes to provide simulation of the rigid pin and bearing mechanism. The inner surface of the upper and lower nodes become rigid surface and connected to the single nodes in the middle of the centre line of the node where boundary conditions are applied. Additionally, one node is created to measure displacement and load which is connected to the upper nodes with equation constraint. For the boundary conditions, every upper and lower nodes of unit chiral lattice can rotate on the edgewise direction, one of the upper nodes freed on Y and X directions, and the other is freed on the only X direction as it seen in Figure 4. Additionally, for the lower nodes, one of them is fixed and other can move only in the lateral direction.

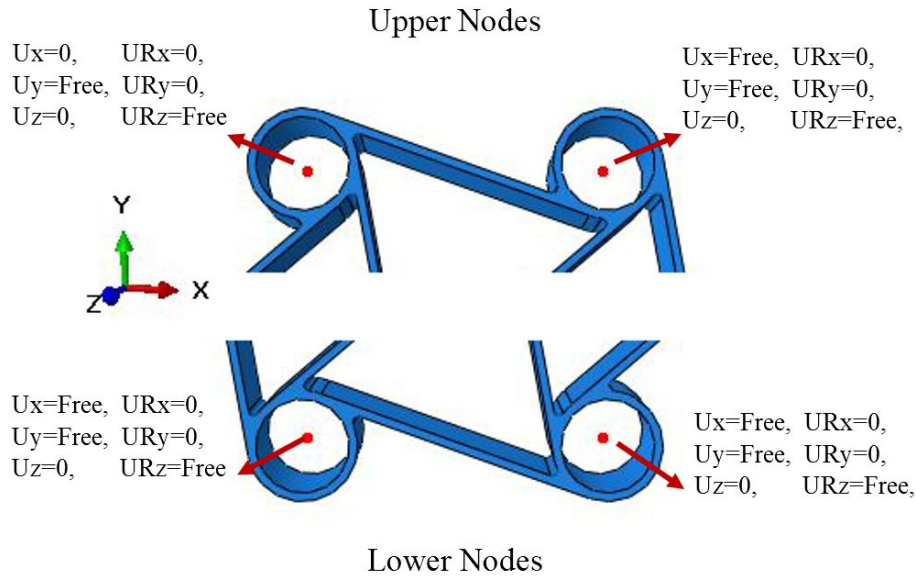


Figure 4: Boundary conditions for chiral unit lattice cell

3 RESULTS

Tensile specimens were produced in the vertical and horizontal direction with Ti6Al4V. The tests were conducted according to ASTM E8. For each direction, five specimens were tested in the as-built conditions. Before the testings, sandblasting was applied to all the specimens to reduce the surface roughness. The average Ra value of the 0-degree and 90-degree specimens $6.74 \mu\text{m}$ and $14.12 \mu\text{m}$, respectively.

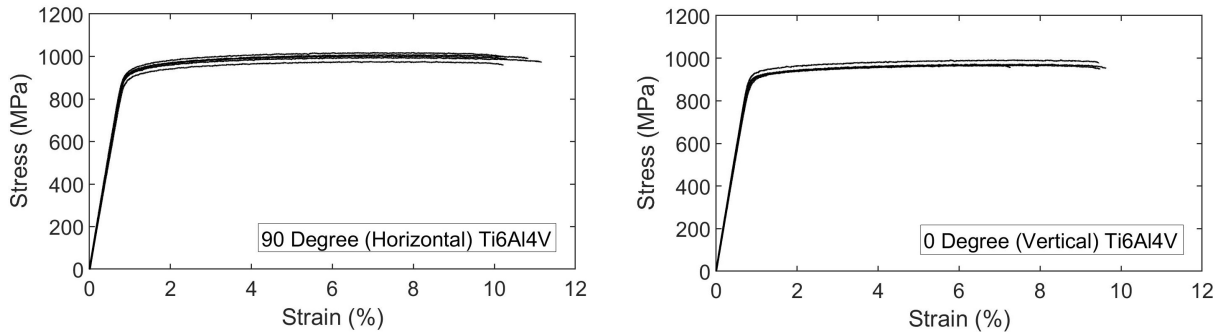


Figure 5: Stress-strain graphs for 0 and 90-degree orientations build specimens

The resulting engineering stress-strain data can be seen in Figure 5. As a result of the investigation the tensile results, Young's moduli that measured have no significant difference according to angular orientation with a value of 110 GPa. The yield stress and ultimate tensile strength values are $922 \pm 2\%$ and $1001 \pm 2.3\%$ for 0-degree orientation production, and $917 \pm 1.9\%$ and $974.7 \pm 1.8\%$ for 90-degree orientation builds, respectively. It is obviously seen from the results the build direction is not a dominating factor for Young's modulus, yields stress and ultimate tensile strength, however considering breaking strain, 0° build exhibits $10.65 \pm 0.58\%$ as the highest value compared to the 90 degree of $8.83 \pm 1.65\%$. As it seen from Table 2, proposed mechanical properties are better than the experimental results. This situation can be explained by the lack of fusion problems caused by EBM production method and material inhomogeneity. As a result of the tensile study, it is understood that Ti4Al6V productions with EBM technology show isotropic elasticity but anisotropic plasticity. In addition, according to variations, 0° build shows consistent mechanical performance comparing the other production degree, this is also the reason of chiral cells were produced where their flatwise direction is parallel to the building plate. Consequently, as a result of experimental studies, inputs for the constitutive equation is obtained, calibrated and imported to FEM codes to represent the behaviour of the material. In the FEM analysis, isotropic elasticity and plasticity were deployed to measure the deformation limit of chiral unit cell without experiencing permanent deformations, degradation or failures. Different boundary condition studies have been conducted, and the change in the boundary conditions increased divergence from the experimental results. As a result of the chiral compressive load tests and FEM analysis, Figure 6 is obtained. In the first two cycles which have 0.5 and 1 mm displacement limits, no permanent deformations were observed. However, in the last cycle having a displacement limit of 1.5 mm, plastic deformation was observed under the compressive load of 1790 N and 1.312 mm displacement.

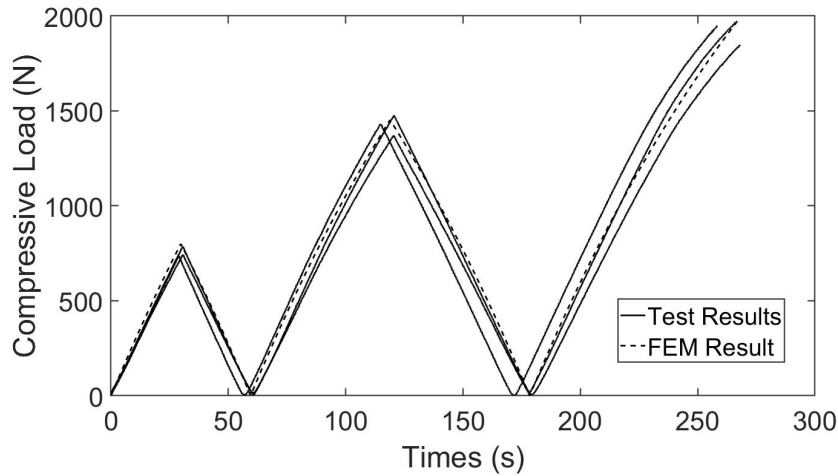


Figure 6: Compressive load profile experimental and FEM results for chiral unit cells

4 CONCLUSIONS

The result of the material characterization of EBM printed Ti6Al4V can be summarized as isotropic elasticity and anisotropic plasticity. In 0° and 90° building orientation, 0° build showed the consistent and better results with the average 10.65% breaking strain value, and 90° showed lower breaking strain which is not preferable for compression applications. Furthermore, chiral lattice cells showed similar reactions under compressive load profile with slight differences which was caused by the displacement control of the testing machine. As a result of compressive load profile, the unit chiral lattice cells have permanent failures under the compressive loads greater than 1790 N in the last cycle of load profile with a displacement of 1.312 mm. In addition, the FEM model including isotropic elasticity and plasticity were validated with the experimental results.

REFERENCES

- [1] Evans, K. E. and Nkansah, I. J. and Hutchinson, I. J. and Rogers, S. C. Molecular network design. *Nature* (1991) **353(6340)**:124–124.
- [2] Prall, D. and Lakes, R. S. Properties of a chiral honeycomb with a Poisson's ratio of $\tilde{f}\tilde{a}\tilde{A}\tilde{T}1$. *International Journal of Mechanical Sciences* (1997) **39(3)**:305–314.
- [3] Spadoni, A. and Ruzzene, M. and Scarpa, F. Dynamic Response of Chiral Truss-core Assemblies. *Journal of Intelligent Material Systems and Structures* (2006) **17(11)**:941–952.
- [4] Zhu, Y., Wang, Z. and Poh, L. H. Auxetic hexachiral structures with wavy ligaments for large elasto-plastic deformation. *Smart Materials and Structures* (2018) **27(5)**:0555001.

- [5] Spadoni, A. and Ruzzene, M. and Scarpa, F. Global and local linear buckling behavior of a chiral cellular structure. *Physica status solidi (b)* (2005) **242(3)**:695–709.
- [6] Bettini, P., Airoidi, A., Sala, G., Landro, L. D., Ruzzene, ., and Spadoni, A. Composite chiral structures for morphing airfoils: Numerical analyses and development of a manufacturing process. *Composites Part B: Engineering* (2010) **41(2)**:133–147.
- [7] Airoidi, A., Crespi, M., Quaranti, G. and Sala, G. Design of a Morphing Airfoil with Composite Chiral Structure. *Journal of Aircraft* (2012) **49(4)**:1008–1019.
- [8] Gibson, L. J. and Ashby, M. F. Cellular Solids: Structure and Properties. (*Cambridge Solid State Science Series*) (1997) **2nd ed.**
- [9] Heintl, P. and Rottmair, A. and Körner, C. and Singer, R. F. Cellular titanium by selective electron beam melting. *Material a Design* (2007) **9(5)**:360–364.
- [10] Arcam AB, (n.d.). Arcam Ti6Al4V Titanium Alloy [Brochure] MÅlndal, Sweden. Retrieved from <http://www.arcam.com/wp-content/uploads/Arcam-Ti6Al4V-Titanium-Alloy.pdf> (Last access 25/06/2019).
- [11] Heintl, P., Rottmair, A., Korner, C. and Singer, R. F. Cellular Titanium by Selective Electron Beam Melting. *Advanced Engineering Materials* (2007) **9(5)**:360–364.
- [12] Spadoni, A. and Ruzzene, M. Numerical and experimental analysis of the static compliance of chiral truss-core airfoils. *Mechanics of Materials and Structures* (2007) **5(2)**:965–981.